

Comparing Field Emission Electron Microprobe to Traditional EPMA of Metallurgical Specimens

D.F. Susan, R.P. Grant, J.M. Rodelas, J.R. Michael, and M.C. Maguire

Sandia National Laboratories, Albuquerque, New Mexico

The use of a thermal field emission electron source and other design changes have significantly increased the resolution of wavelength dispersive spectroscopy (WDS) electron probe microanalysis (EPMA), especially in the 5-8kV range of accelerating voltage.[1,2] The analysis of particles/phases as small as 200 nm in diameter has been documented for geological and meteoritical specimens and a similar analytical volume was shown in a Sn-Ag solder alloy.[1,2] The present work highlights other examples of field emission EPMA for the analysis of fine-scale metallurgical microstructures. Features too small for traditional EPMA, such as fine-scale lamellar transformations and microsegregation in solidification microstructures, can now be analyzed successfully with FE-EPMA. High resolution is obtained while simultaneously covering a long linescan length or a relatively large area for mapping.

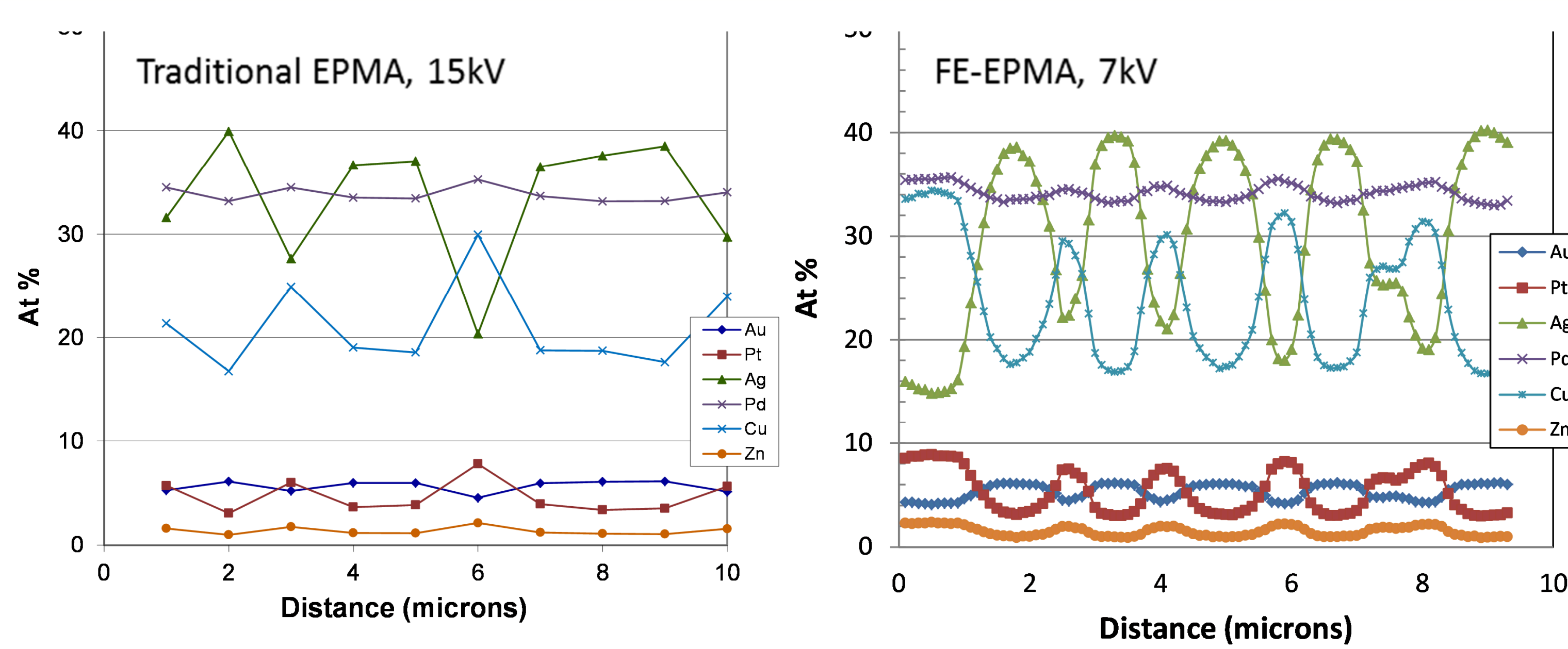


Fig. 1. (top) FE-EPMA elemental maps showing Ag concentration in a multicomponent precious metal alloy. (bottom) EPMA linescan through the lamellar structure obtained with a traditional EPMA instrument and an FE-EPMA linescan at 7kV on a JEOL JXA-8530F.

Figure 1 displays a two-phase lamellar structure formed in a multi-component precious metal alloy. The individual layers range from sub-micron to about a micron in width. A traditional EPMA line scan of six elements is shown with typical 15kV accelerating voltage and one-micron spacing of analysis points. With conventional microprobe, the lamellar phase compositions are just barely discerned; silver-rich and copper-rich phases are alternating in the microstructure. In some places only one analysis point is contained within a phase and there is likely significant overlap of analyzed volume from the surrounding phases. The Pd concentration appears relatively flat and the minor constituents of Au, Pt, and Zn show slight fluctuations in each phase but it is difficult to quantify the compositional changes.

In the right-hand plot, an FE-EPMA line scan of similar length is exhibited, obtained on a JEOL JXA-8530F at 7kV with 0.1 micron spacing. The lamellar phase compositions are now easily determined and the segregation of the minor elements between the two phases is clearly evident as well. The data can be used for phase diagram analysis and to characterize the lamellar discontinuous precipitation mechanism.[3]

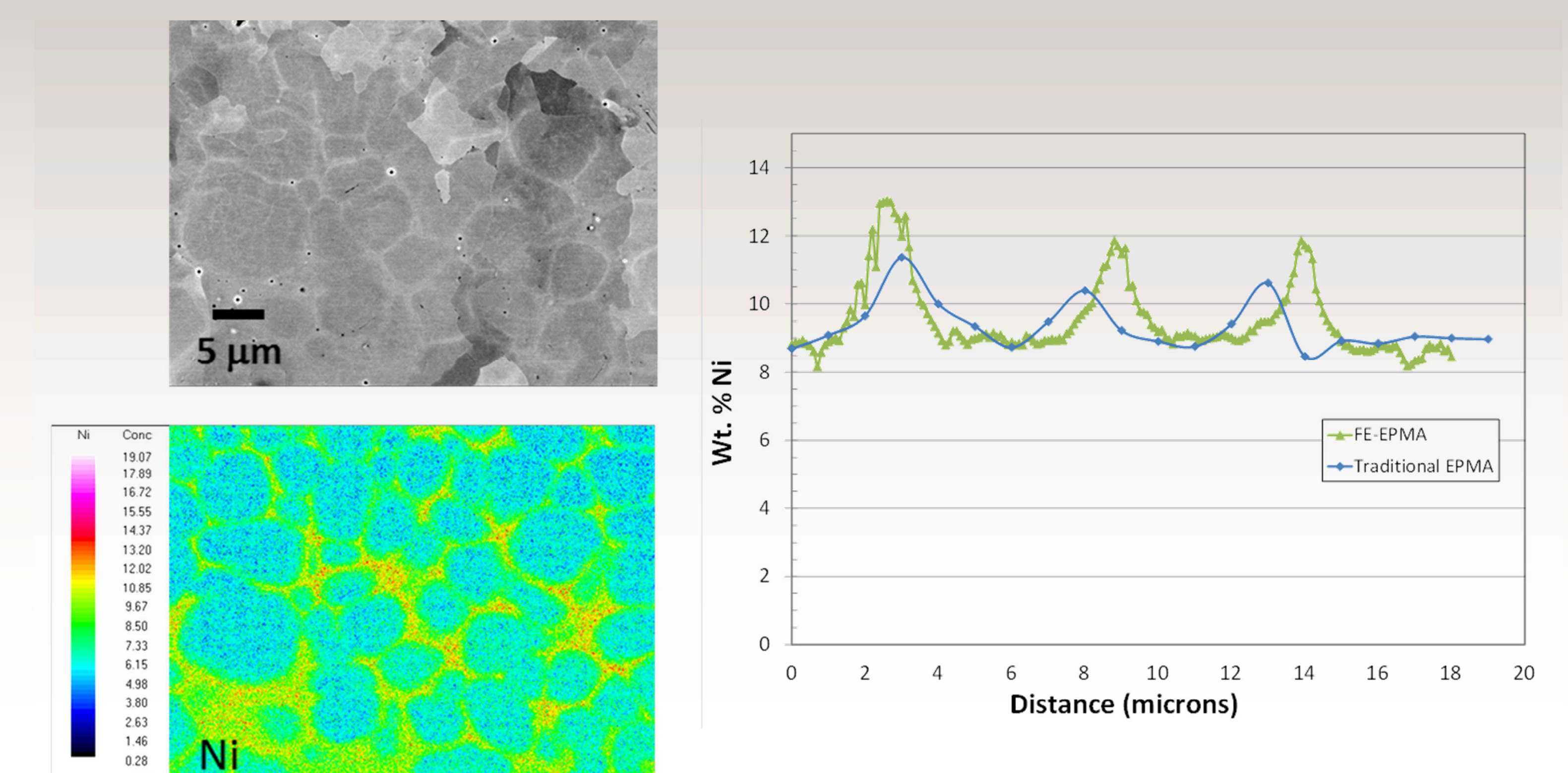


Fig. 2. (left) BSE photo and Ni elemental map from a stainless steel weld microstructure. (right) EPMA and FE-EPMA linescans of Ni concentration.

In Fig. 2, FE-EPMA analysis of an austenitic stainless steel weld structure is presented. As shown in the elemental map of Ni, the FE-EPMA is able to resolve fine-scale intercellular segregation of Ni in the weld structure. In the linescan plot, the FE-EPMA results are compared to a traditional EPMA trace. Although the traditional EPMA trace is able to show the general segregation pattern, it does not accurately determine the peaks in Ni concentration. Again, only a few data points are collected in the peaks and valleys of composition. Note the two traces were taken in slightly different locations so the interdendritic patterns do not exactly align spatially. Figure 3 compares lower magnification Ni maps taken with traditional EPMA with 1 micron step size and FE-EPMA with 100 nm step size. Traditional mapping shows essentially a uniform noisy field of Ni X-ray signal while the high resolution mapping reveals, at least qualitatively, the cellular dendritic solidification structure within the laser weld.

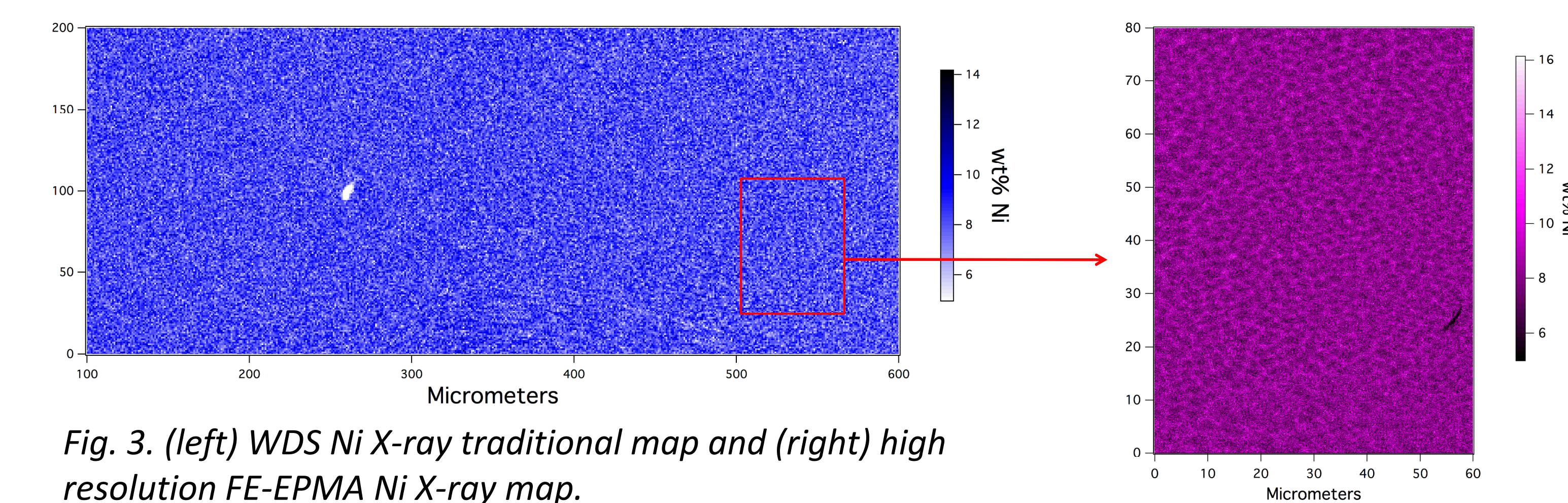


Fig. 3. (left) WDS Ni X-ray traditional map and (right) high resolution FE-EPMA Ni X-ray map.

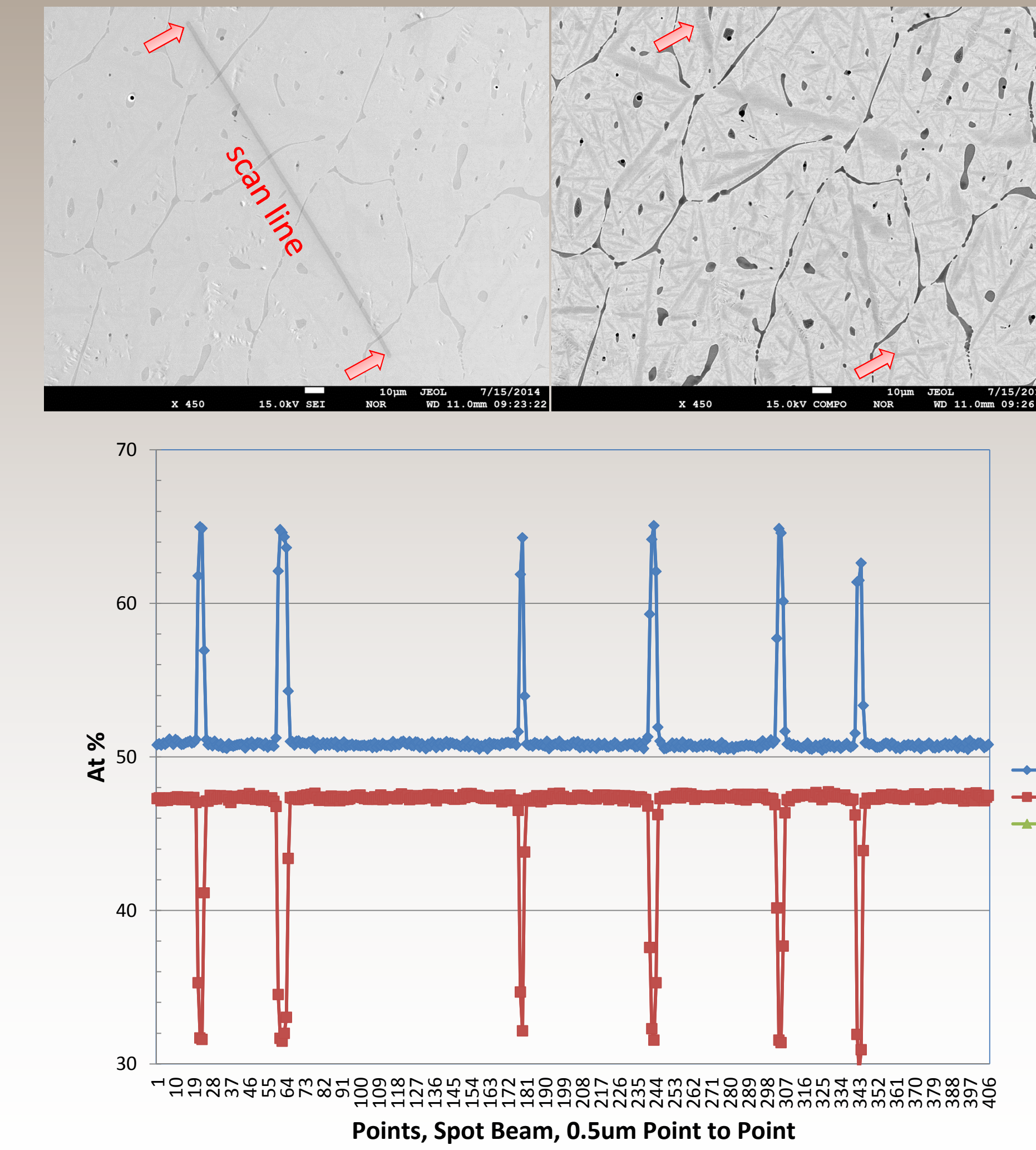


Fig. 4. SE and BSE photos of a Ti-rich NiTi alloy in the cast plus homogenized condition. Traditional EPMA/WDS trace showing Ti-rich/Ni-lean (Ti_2Ni) interdendritic regions.

while the FE-EPMA, with 100nm scan steps, contains as many as ten data points within the Ti-rich interdendritic regions (Fig. 5). Thus, with FE-EPMA, robust compositional analyses of fine-scale solidification microstructures can be achieved with unambiguous analysis volumes, i.e. little or no phase overlap.

The examples highlighted in this work show that FE-EPMA can be a powerful analytical tool for studies of solidification/casting and welding as well as other metallurgical processes that produce fine-scale multiphase structures or compositional fluctuations.

Another example of traditional EPMA vs. FE-EPMA is exhibited in Figs. 4 and 5 for a slightly Ti-rich NiTi shape memory alloy in the as-cast plus homogenized condition. Secondary and backscatter electron images show the multiphase dendritic microstructure and the locations of the EPMA line scans. The interdendritic regions are Ti-rich and Ni-lean compared to the alloy matrix and identified as Ti_2Ni (with oxygen substitution, not shown here). The traditional EPMA scan contains only one or two data points fully contained within the thin interdendritic regions (Fig. 4)

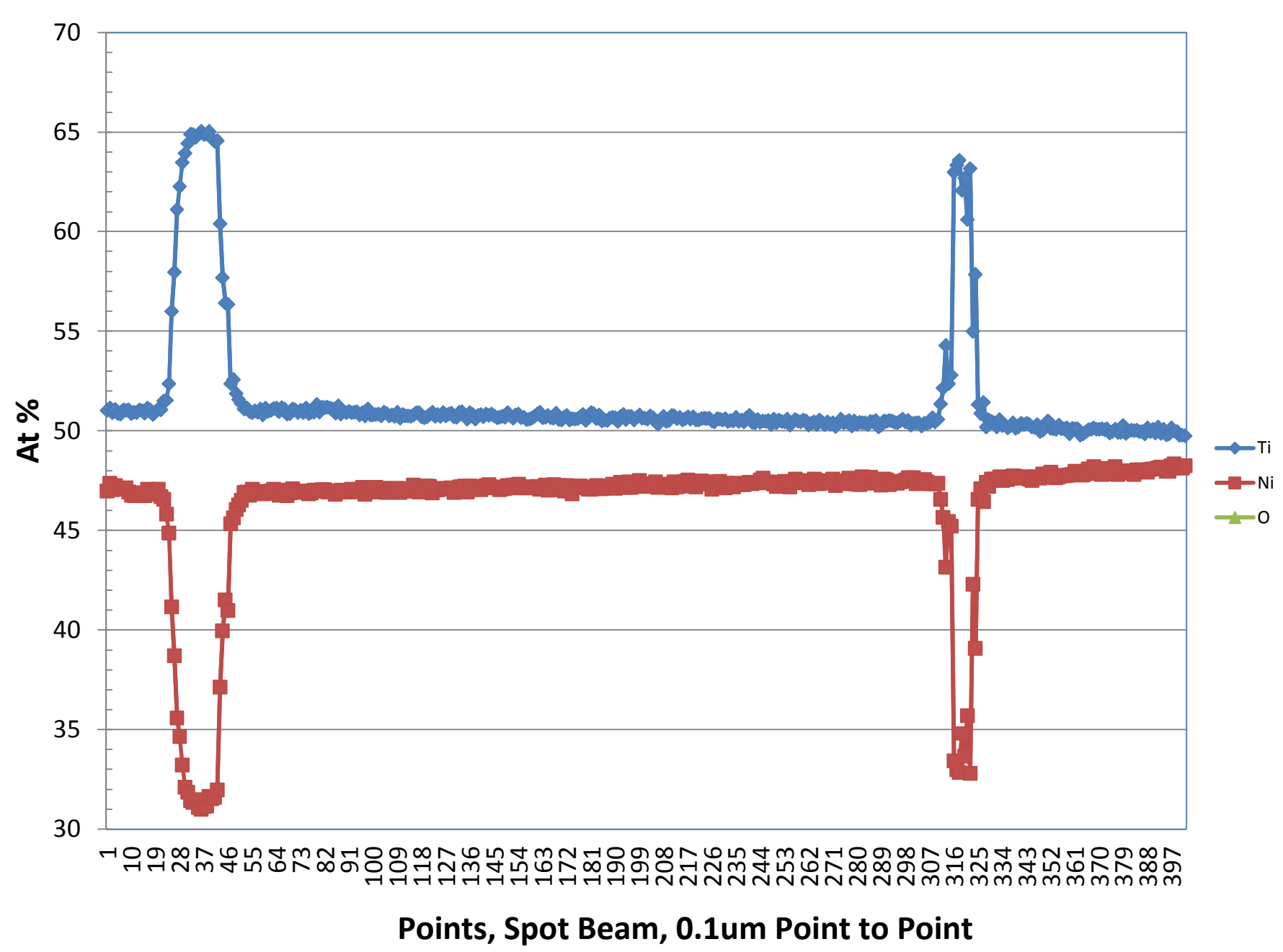
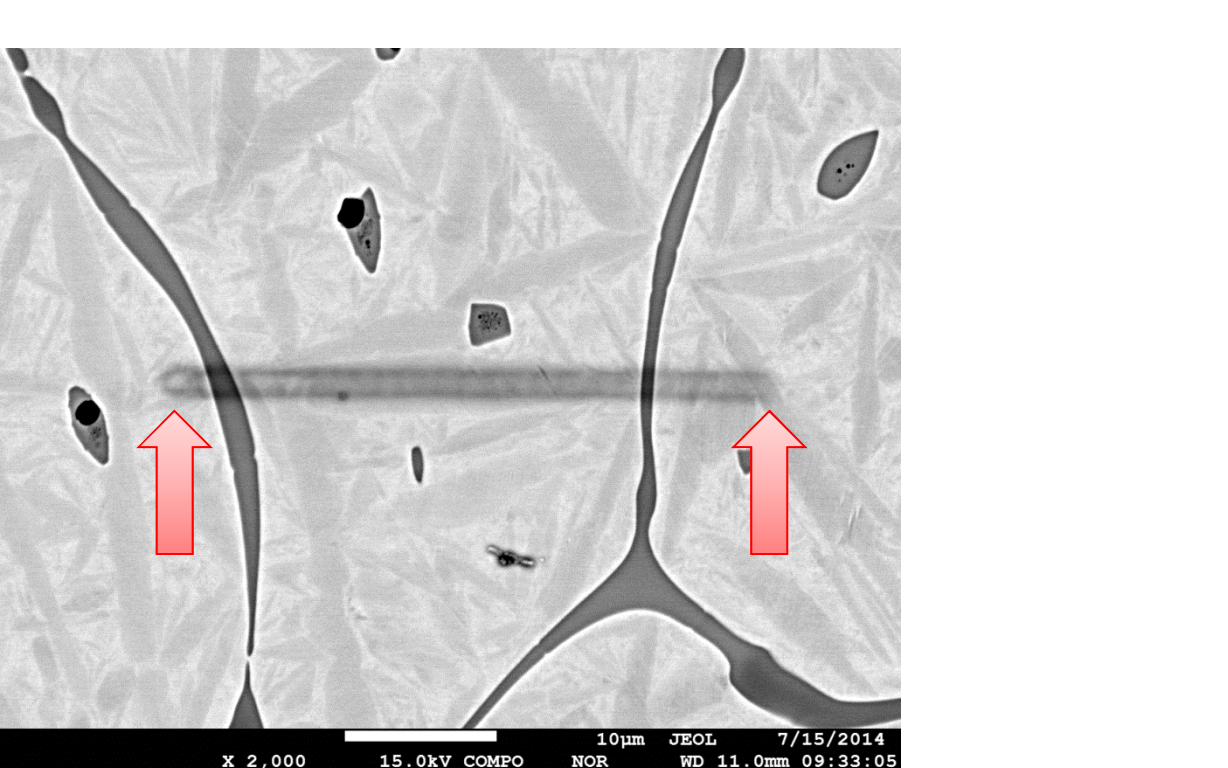


Fig. 5. BSE photo of NiTi alloy in the cast plus homogenized condition. FE-EPMA/WDS trace showing Ti-rich/Ni-lean (Ti_2Ni) interdendritic regions.